Article:

Scott, Neil W.J., Ford, Mark J., Husbands, David R. et al. (2 more authors) (2021) Reactivity of a Dinuclear PdIComplex [Pd2(μ-PPh2)(μ2-OAc)(PPh3)2] with PPh3:Implications for Cross-Coupling Catalysis Using the Ubiquitous Pd(OAc)2/nPPh3Catalyst System. Organometallics. pp. 2995-3002. ISSN 0276-7333

https://doi.org/10.1021/acs.organomet.1c00347

ORGANOMETALLICS

pubs.acs.org/Organometallics Article

Reactivity of a Dinuclear Pd^I Complex $[Pd_2(\mu\text{-}PPh_2)(\mu_2\text{-}OAc)(PPh_3)_2]$ with PPh_3: Implications for Cross-Coupling Catalysis Using the Ubiquitous $Pd(OAc)_2/nPPh_3$ Catalyst System

Neil W. J. Scott, Mark J. Ford, David R. Husbands, Adrian C. Whitwood, and Ian J. S. Fairlamb*

Cite This: *Organometallics* 2021, 40, 2995−3002 Read Online

ACCESS | Metrics & More | Article Recommendations | Supporting Information

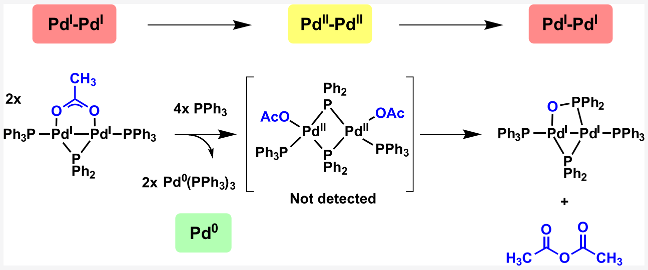

ABSTRACT: $[Pd^I_2(\mu\text{-}PPh_2)(\mu_2\text{-}OAc)(PPh_3)_2]$ is the reduction product of $Pd^{II}(OAc)_2(PPh_3)_2$, generated by reaction of '$Pd(OAc)_2$' with two equivalents of PPh_3. Here, we report that the reaction of $[Pd^I_2(\mu\text{-}PPh_2)(\mu_2\text{-}OAc)(PPh_3)_2]$ with PPh_3 results in a nuanced disproportionation reaction, forming $[Pd^0(PPh_3)_3]$ and a phosphinito-bridged Pd^I-dinuclear complex, namely $[Pd^I_2(\mu\text{-}PPh_2)\{\kappa_2\text{-}P,O\text{-}\mu\text{-}P(O)Ph_2\}(\kappa\text{-}PPh_3)_2]$. The latter complex is proposed to form by abstraction of an oxygen atom from an acetate ligand at Pd. A mechanism for the formal reduction of a putative Pd^{II} disproportionation species to the observed Pd^I complex is postulated. Upon reaction of the mixture of $[Pd^0(PPh)_3]$ and $[Pd^I_2(\mu\text{-}PPh_2)\{\kappa_2\text{-}P,O\text{-}\mu\text{-}P(O)Ph_2\}(\kappa\text{-}PPh_3)_2]$ with 2-bromopyridine, the former Pd^0 complex undergoes a fast oxidative addition reaction, while the latter dinuclear Pd^I complex converts slowly to a tripalladium cluster, of the type $[Pd_3(\mu\text{-}X)(\mu\text{-}PPh_2)_2(PPh_3)_3]X$, with an overall 4/3 oxidation state *per* Pd. Our findings reveal complexity associated with the precatalyst activation step for the ubiquitous '$Pd(OAc)_2$'/$nPPh_3$ catalyst system, with implications for cross-coupling catalysis.

Pd^I dinuclear complexes are increasingly being adopted as effective and distinctive cross-coupling precatalysts.[1−8] The Schoenebeck group has demonstrated that such complexes, and their derivatives, display unique reactivity, particularly with respect to controllable chemoselectivity in cross-coupling reactions, which has very recently been reviewed.[9] Building on the important work on the activation of '$Pd(OAc)_2$' by Amatore and Jutand,[10−12] our group recently discovered that the phosphido-bridged Pd^I-dinuclear complex $[Pd^I_2(\mu\text{-}PPh_2)(\mu_2\text{-}OAc)(PPh_3)_2]$ **1** forms via *trans*-$Pd^{II}(OAc)_2(PPh_3)_2$ in the reaction between $[Pd^{II}_3(OAc)_6]$ and exactly 6 equiv of PPh_3 (where the $Pd{:}PPh_3 = 1{:}2$). This is a precatalytic $Pd{:}PPh_3$ ratio often employed as an effective catalyst system in synthetic chemistry applications. Recently, dinuclear Pd^I complexes have been shown to form by reaction between $Pd(OAc)_2$ and dialkylbiaryl phosphines.[13−15] As part of an investigation into its role in cross-coupling catalysis, the reactivity of **1** with electrophilic organohalides was conducted.[16] $[Pd^I_2(\mu\text{-}PPh_2)(\mu_2\text{-}OAc)(PPh_3)_2]$ **1** was found to activate organohalides at room temperature to afford tripalladium clusters, of the type $[Pd_3(\mu\text{-}X)(\mu\text{-}PPh_2)_2(PPh_3)_3]$-X, in addition to more commonly anticipated oxidative addition Pd^{II} products (Figure 1a). The finding, while intriguing for catalytic cross-coupling, is underpinned by a significant history of $[Pd_3(X)(PPh_2)_2(PPh_3)_3]X$ clusters dating back to their synthesis and characterization in the late 1960s.[17−20]

The reactivity of another Pd^I dinuclear complex, $[Pd(\mu\text{-}Br)(P^tBu_3)]_2$, toward 3 equiv of $PtBu_3$ was reported by Colacot and Schoenebeck et al., which afforded $[Pd^0(PtBu_3)_2]$ as the predominant product (Figure 1b).[2]

We considered that another species (e.g., Pd^{II}) might accompany Pd^0 in this type of reaction, at least transiently, as the apparent process is of a disproportionative nature. Indeed, controlled catalyst activation of dinuclear Pd^I complexes to Pd^0 complexes by disproportionation has been proposed as a rationale for their exceptional reactivity.[21−23] Hazari et al. rationalized that the in situ-formed NHC-containing dinuclear

Received: June 11, 2021
Published: August 19, 2021

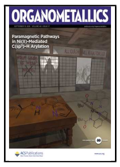

https://doi.org/10.1021/acs.organomet.1c00347
Organometallics 2021, 40, 2995−3002

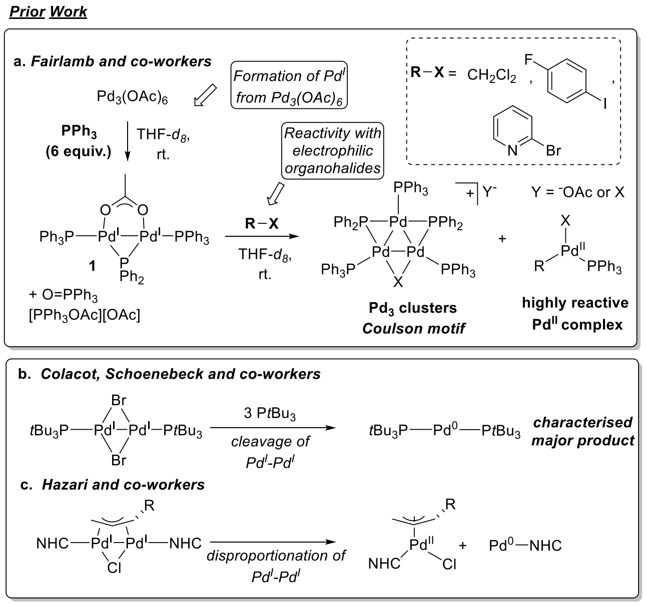

Figure 1. (a) Formation of $[Pd^I_2(\mu\text{-}PPh_2)(\mu_2\text{-}OAc)(PPh_3)_2]$ complex **1** and reactivity with organohalides. (b, c) Examples of reactivity of $Pd^I{-}Pd^I$ dinuclear complexes.

complex$(\mu\text{-allyl})(\mu\text{-Cl})Pd_2(NHC)_2$ was activated for catalysis via disproportion to $Pd^{II}Cl(\eta^3\text{-allyl})(NHC)$ and $[Pd^0{-}NHC]$ (Figure 1c, NHC = N-heterocyclic carbene ligand *I*Pr).[24] Thus, we continued to pursue uncovering the distinctive reactivity of Pd^I-dinuclear complexes so that the implications for cross-coupling catalysis can be more broadly understood. Herein, we report that addition of PPh_3 to $[Pd^I_2(\mu\text{-}PPh_2)(\mu_2\text{-}OAc)(PPh_3)_2]$ **1**, induces disproportionation and subsequent conversion to a dinuclear Pd^I, namely $[Pd^I_2(\mu\text{-}PPh_2)\{\kappa_2\text{-P,O-}\mu\text{-}P(O)Ph_2\}(\kappa\text{-}PPh_3)_2]$, in addition to $[Pd^0(PPh_3)_3]$. These two different species exhibit distinct reactivity profiles toward 2-bromopyridine in forming either mononuclear Pd species or higher order Pd_3 cluster species. The portioning between these two types of species is important for the field of cross-coupling catalysis to consider.

■ RESULTS AND DISCUSSION

Reactivity of $[Pd_2(\mu\text{-}PPh_2)(\mu_2\text{-}OAc)(PPh_3)_2]$ with PPh_3. In our first reaction, $[Pd^I_2(\mu\text{-}PPh_2)(\mu_2\text{-}OAc)(PPh_3)_2]$ **1** was treated with one equivalent of PPh_3 in THF-d_8 at room temperature. After ca. 30 min, ^{31}P NMR spectral analysis revealed the formation of new species (Figure 2b), which could be compared with an authentic sample of **1** (Figure 2a). A phosphorus triplet signal, at δ_P 199.6, was assigned as the diphenylphosphido signal of unreacted **1**. A loss of resolution of the triplet was evident, as well as a slight downfield change in chemical shift, δ_P 199.1 → 199.6 ppm (Figure 2b). Two new well-resolved resonances appeared at δ_P 122.6 and 77.3 ppm, with doublet (*d*) and doublet of doublets (*dd*) multiplicities, respectively, which were found to integrate in a 1:1 ratio (hereafter species **2**; a discussion of coupling constants is found in the text below). A major, broad resonance at δ_P 23.9 ppm was evident. Two broad resonances at approximately δ_P 26 and 15 ppm were also observed.

Upon reaction of **1** with two equivalents of PPh_3, further reaction progression was evident by ^{31}P NMR spectroscopic analysis after ca. 0.5 h reaction time (Figure 2c). The complete loss of **1** was seen by the disappearance of its phosphido ^{31}P NMR resonance. Low-field resonances at δ_P 122.6 and 77.3 ppm, which were again present, broaden out, with both appearing as doublets (supporting formation of a new species **2**). The major, broad resonance appeared to shift marginally upfield from δ_P 23.9 → 23.1 ppm, which is $[Pd^0(PPh_3)_3]$. Broadened peaks at ∼ δ_P 25.6 and 15.6 ppm were also present, indicating PPh_3 exchange taking place in the presence of additional phosphine. Treatment of the reaction mixture with 10 equiv of PPh_3 resulted in disappearance of these broad resonances and migration of the major singlet to δ_P 7.6 ppm (externally referenced to H_3PO_4(aq) 85% w/w) (see Supporting Information). The migration of this signal upfield (toward the chemical shift of free PPh_3) is consistent with the reported behavior of $[Pd^0(PPh_3)_n]$ toward additional PPh_3.[10,16]

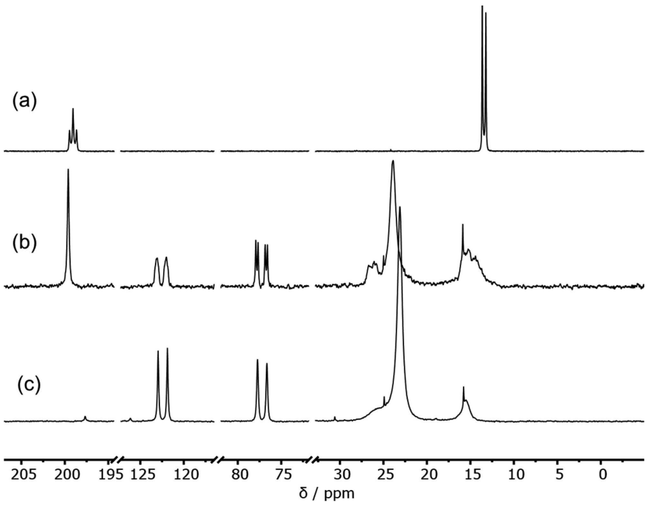

Figure 2. $^{31}P\{^1H\}$ NMR (THF-d_8, 25 °C, 203 MHz) showing reaction of $[Pd^I_2(\mu\text{-}PPh_2)(\mu_2\text{-}OAc)(PPh_3)_2]$ **1** with nPPh_3. (a) Authentic **1**; (b) $[Pd^I_2(\mu\text{-}PPh_2)(\mu_2\text{-}OAc)(PPh_3)_2]$ **1** + 1 equiv of PPh_3 after 0.5 h; (c) $[Pd^I_2(\mu\text{-}PPh_2)(\mu_2\text{-}OAc)(PPh_3)_2]$ **1** + 2 equiv of PPh_3 after 0.5 h. Note: the spectral window has been shortened, as shown by the double diagonal lines on the chemical shift scale line.

A bright red-orange crystal of this new species **2** was grown by carefully layering pentane onto a cooled THF solution of the postreaction mixture of $[Pd^I_2(\mu\text{-}PPh_2)(\mu_2\text{-}OAc)(PPh_3)_2]$ **1** and two equivalents of PPh_3 (stored at −18 °C for ca. 2 days). The crystal was subjected to single-crystal X-ray diffraction analysis which enabled the structural elucidation of this new species to be determined (Figure 3). It is important to note that the asymmetric unit of crystal structural data contains two half complexes of **2**, each of which are disordered about a center of inversion.

The single-crystal X-ray diffraction structure of $[Pd_2(\mu\text{-}PPh_2)\{\kappa_2\text{-P,O-}\mu\text{-}P(O)Ph_2\}(\kappa\text{-}PPh_3)]$ **2** shows that the P, O, and Pd atoms all lie within approximately the same plane (Figure 3). The Pd atoms are stabilized by bridging μ-phosphido and μ_2-phosphinito ligands. The Pd1−P4 and the Pd2−O1 bond distances [2.328(3) and 2.150(7) Å, respectively] are significantly less than the sum of the van der Waals radii of the respective atoms, indicating that both O and P atoms of the diphenylphosphinito ligand are bonded to Pd (see DFT calculations later). The Pd1−Pd2 interatomic distance was determined to be 2.5680(10) Å, in-keeping with $Pd^I{-}Pd^I$ bond lengths of similar Pd^I dinuclear complexes.[15,16,25−27] The P−O bond of the diphenylphosphinito

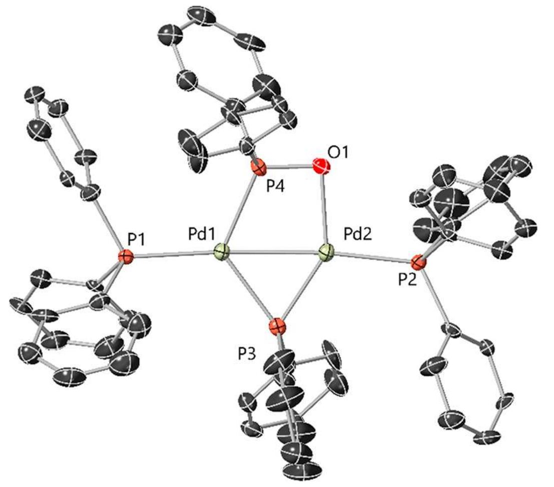

Figure 3. Structure of $[Pd_2(\mu\text{-}PPh_2)\{\kappa_2\text{-}P,O\text{-}\mu\text{-}P(O)Ph_2\}(\kappa\text{-}PPh_3)]$ (2), obtained via X-ray diffraction of a single crystal grown from THF-d_8 reaction solution of $[Pd^I_2(\mu\text{-}PPh_2)(\mu_2\text{-}OAc)(PPh_3)_2]$ 1 with two equivalents of PPh_3. Selected interatomic distances /Å: Pd1−Pd2 = 2.5680(10), Pd1−P1 = 2.360(9) Pd2−P2 = 2.275(9), Pd1−P3 = 2.316(3), Pd2−P3 = 2.210(3), P1−P4 = 2.328(3), P4−O1 = 1.550(8), P2−O1 = 2.150(7). Selected interatomic angles /°: Pd1−P3−Pd2 = 69.093, Pd1−Pd2−O1 = 86.162, Pd2−O1−P4 = 93.688. Note: a single molecule from the asymmetric unit cell is shown only for clarity. H-atoms not shown.

ligand [P4−O1 = 1.550(8) Å] has some double bond-character at 1.479(2) Å),[28] which falls within the region seen for another bridging diphenylphospinito dinuclear Pd^I complex reported by Matt et al.[29] The structure of **2** is desymmetrized along the $Ph_3P(P3)-Pd(1)-Pd(2)-PPh_3(P4)$ bond axis, with the Pd1−P3 interaction being approximately 4% longer than that of P2−P4. It is pertinent to mention that a related PCy_2-bridged-Pt complex is known.[30a]

Mass spectral analysis (+ve mode) of the postreaction solution provided further evidence for the species formed under the reaction conditions. ESI- and LIFDI-MS analysis were complementary in confirming the presence of $[Pd_2(\mu\text{-}PPh_2)\{\kappa_2\text{-}P,O\text{-}\mu\text{-}P(O)Ph_2\}(\kappa\text{-}PPh_3)]$ **2** as the pseudomolecular ion $[M + H]^+$ (exact mass m/z = 1123.20) (Figure 4a, i) and $[M]^{\cdot+}$ (exact mass m/z = 1122.09), respectively, with the correct isotopic distribution}. LIFDI-MS analysis indicated the presence of an ion at m/z = 982.18; this is equal to the exact mass of $[Pd^0(PPh_3)_3]$, detected as $[Pd(PPh_3)_3]^{\cdot+}$ (i.e., the radical cation), with the correct isotopic distribution (Figure 4a, i). A low-temperature $^{31}P\{^1H\}$ NMR spectrum of a sample from the reaction of **1** with two equivalents of PPh_3 (173 K, −100 °C, THF-d_8, 203 MHz) was recorded (Figure 4b, i). Two low-field resonances at δ_P 123.1 and 75.6 ppm (observed as doublets at 298 K) and two new, high-field PPh_3-type resonances at δ_P 27.6 and 12.0 ppm were resolved (previously broad at 298 K), revealing fine coupling between four peaks, each resolving as *ddd* peak multiplicities, giving information important for the complete assignment of the solution

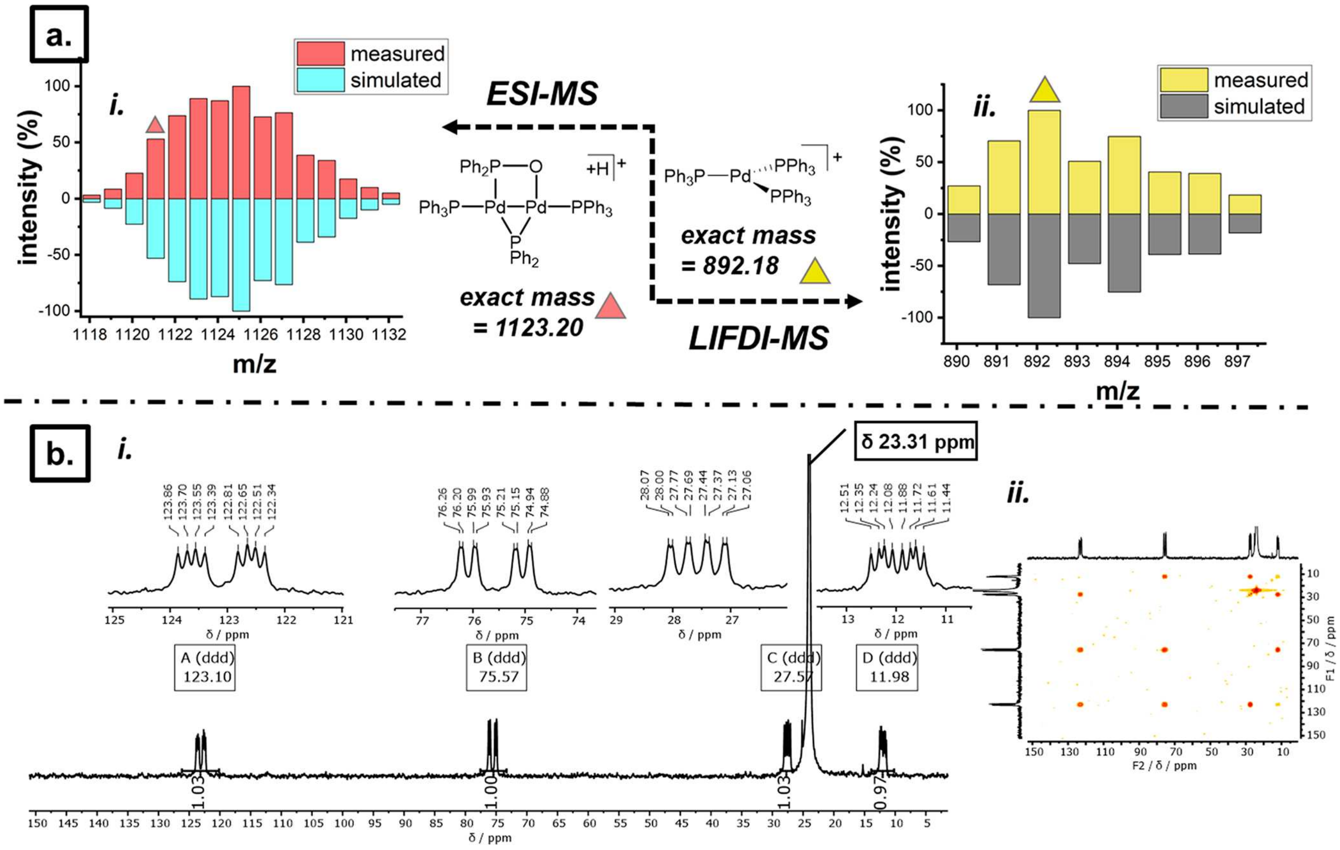

Figure 4. Key characterization data obtained from the postreaction solution (THF-d_8), containing the products of the reaction between $[Pd^I_2(\mu\text{-}PPh_2)(\mu_2\text{-}OAc)(PPh_3)_2]$ **1** and two equivalents of PPh_3. (a) Mass spectral data for ions detected in the reaction solution; $[Pd_2(\mu\text{-}PPh_2)\{\kappa_2\text{-}P,O\text{-}\mu\text{-}P(O)Ph_2\}(PPh_3)_2]^{+}$, detected by ESI-MS and $[Pd^0(PPh_3)_3]$ detected by LIFDI-MS (right). (b) 1D $^{31}P\{^1H\}$ and 2D $^{31}P-^{31}P\{^1H\}$ COSY NMR spectra (202.5 MHz, CD_2Cl_2), recorded at 173 K of the postreaction solution.

structure of **2**. Each phosphorus resonance integrates in a 1:1:1:1 ratio. The P−P spin coupling constants (in Hz) for each resonance are collated in Table 1. The four ^{31}P resonances were assigned to the four phosphorus atoms as present in the single-crystal X-ray diffraction structure (Figure 3; **2**,Table 1). A large $^{2}J_{PP}$ coupling between the two low-field resonances **A** and **B** (217 Hz) is consistent with the *trans*-arrangement of the phosphinito and phosphide ligands spanning the Pd^{I}−Pd^{I} fragment. Likewise, the large $^{3}J_{PP}$ coupling constant observed between high-field phosphine-type resonances (131.5 Hz, **C** and **D**) is consistent with a *trans*-configuration.

Table 1. J_{PP} Coupling Constants (in Hz) for each ^{31}P{^{1}H} Resonance in 2, Recorded at Low Temperature (202.5 MHz, THF-d_8, 173 K)

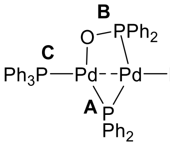

2

	δ/ppm			
	123.1	75.6	27.6	12.0
label	**A**	**B**	**C**	**D**
A	0	217.2	61.5	33.6
B	217.2	0	15.8	55.8
C	61.5	15.8	0	131.5
D	33.6	55.8	131.5	0

The smallest $^{3}J_{PP}$ coupling constant observed (15.8 Hz, between **B** and **C**) fits with a *cis*-configuration, coupling through oxygen, between the phosphinito resonance (**B**) and one of the adjacent phosphines (**C**). A larger $^{2}J_{PP}$ coupling constant (55.8 Hz) was measured between the phosphido resonance (**B**) and the adjacent phosphine (**D**). The complete connectivity of the phosphorus atoms was confirmed by ^{31}P−^{31}P COSY-NMR spectral analysis (Figure 4). Hence, the ^{31}P NMR spectrum of $[Pd_2(\mu\text{-}PPh_2)\{\kappa_2\text{-}P,O\text{-}\mu\text{-}P(O)Ph_2\}(\kappa\text{-}PPh_3)]$ **2** in THF-d_8 agrees with the connectivity suggested by the single-crystal X-ray diffraction structure (Figure 3), along with the cation detected by MS analysis, providing strong evidence that the structure present in THF-d_8 solution is **2**, as in the solid-state. In addition to **2**, the presence of $[Pd^{0}(PPh_3)_3]$ is supported by its detection (radical cation) by LIFDI-MS analysis of the reaction solution.

An additional piece of the jigsaw enabling full reaction mapping was provided by analysis of the ^{1}H and ^{13}C NMR spectra of the reaction mixtures (500, 125.8 MHz, respectively, in THF-d_8). For example, resonances at δ_H 2.15 ppm and δ_C 166.1 and 20.9 ppm suggested formation of acetic anhydride (confirmed by comparison with an authentic sample). Integration of the ^{1}H NMR spectrum confirmed the ratio of $[Pd_2(\mu\text{-}PPh_2)\{\kappa_2\text{-}P,O\text{-}\mu\text{-}P(O)Ph_2\}(\kappa\text{-}PPh_3)]$ **2**:Ac_2O to be 1:1 (see Supporting Information).

Taken together, these data indicate that the room temperature reaction between $[Pd^{I}_2(\mu\text{-}PPh_2)(\mu_2\text{-}OAc)(PPh_3)_2]$ **1** and two equivalents of PPh_3 cleanly affords $[Pd_2(\mu\text{-}PPh_2)\{\kappa_2\text{-}P,O\text{-}\mu\text{-}P(O)Ph_2\}(\kappa\text{-}PPh_3)]$ **2** and $[Pd^{0}(PPh_3)_3]$, as evidenced by ^{31}P NMR and MS analysis, along with acetic anhydride. A mechanistic scheme describing how the events leading to the formation of **2**, $[Pd^{0}(PPh_3)_3]$, and Ac_2O have occurred is shown in Figure 5. The presence of acetic anhydride and **2**, as the other products of this type of process, gives clues as to what has happened to the resulting putative Pd^{II} fragment **I** that formed during disproportionation of the starting dinuclear Pd^{I} complex **1** (Figure 5). We propose that acetic anhydride forms by acyl transfer to acetate at Pd, with loss of one oxygen atom to phosphorus, in forming the phosphinito ligand. In this system, under rigorous Schlenk conditions, acetic anhydride can only derive from the acetate ligands of **2**.

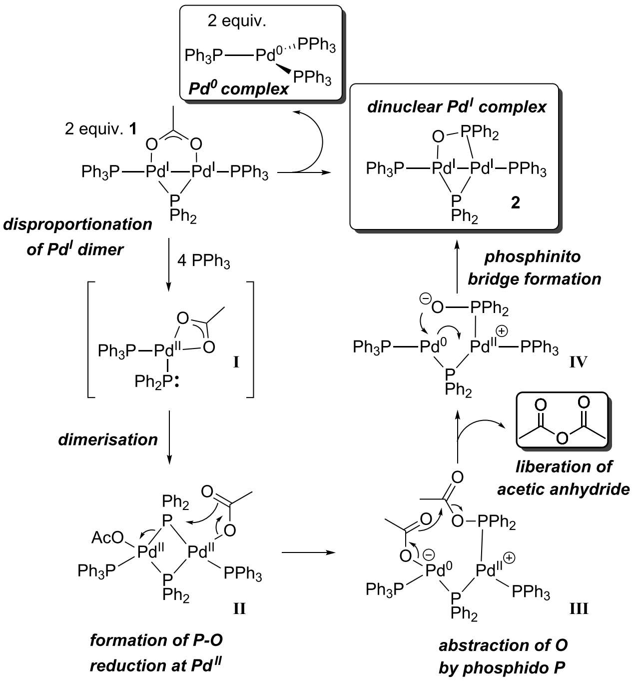

Figure 5. Proposed mechanism for the disproportionation reaction leading to formation of $[Pd^{I}_2(\mu\text{-}PPh_2)\{\kappa_2\text{-}P,O\text{-}\mu\text{-}P(O)Ph_2\}(\kappa\text{-}PPh_3)_2]$ (**2**) and $[Pd^{0}(PPh_3)_3]$.

It is important to acknowledge that a dinuclear Pt^{II} complex containing a P,O-bridging phosphinito ligand was formed from the reaction of a higher oxidation state dinuclear Pt^{III} species with hydroxide anion, involving nucleophilic attack of hydroxide at the electrophilic Pt^{III} center.[30b] Under our conditions, hydroxide anion is not generated (we would expect Ac_2O to be converted to acetic acid, which was not observed).

The transient stability of Pd^{II} fragment **I** could be conferred by the acetate ligand adopting an η_2-OAc binding mode;[31] however, dimerization could then occur rapidly via bridging interactions from nucleophilic κ_2-diphenylphosphido ligands,[32] affording dinuclear Pd^{II} complex **II**. The proximal relationship of the acetate and phosphide ligands sets-up a favored P−O bonding interaction leading to a formal reduction at Pd from two to zero. Subsequent nucleophilic attack on the carbonyl group linked to the phosphorus(V) center in **III** leads to the generation of acetic anhydride, leaving one oxygen atom connected to phosphorus in **IV**, enabling a bridging coordination mode of O to Pd. Thus, the characterized $[Pd^{I}_2(\mu\text{-}PPh_2)\{\kappa_2\text{-}P,O\text{-}\mu\text{-}P(O)Ph_2\}(\kappa\text{-}PPh_3)_2]$ complex **2** is then formed. The redox process is driven by the formation of a strong P−O bond, much like in the formation of Pd^{0} from phosphine-ligated Pd^{II} acetate complexes (vide supra).[10,12] The reaction of a Pd^{I} dimer by disproportionation, followed by a reduction at Pd is not unprecedented. Disproportionation followed by reduction at the Pd^{II} fragment has been observed by Figueroa et al., but in that case, full reduction of an isopropoxide-bridged, bulky isocyanide-stabilized Pd^{I} dinuclear complex to Pd^{0} occurred, ultimately leading to the formation of a Pd^{0} trimer. Interestingly, acetone and propene were observed by Figueroa et al. as oxidized biproducts, and the Pd^{0} fragments combined to form a Pd_3 cluster complex.[33]

In subsequent experiments, we found that a minor new species crystallized from a reaction mixture where **2** was the major species (grown by layering a THF postreaction solution with hexane, which was stored under Ar at −18 °C). A single crystal was subjected to X-ray diffraction analysis, showing it to be yet another novel Pd^{I} dinuclear complex (**3**) (Figure 6).

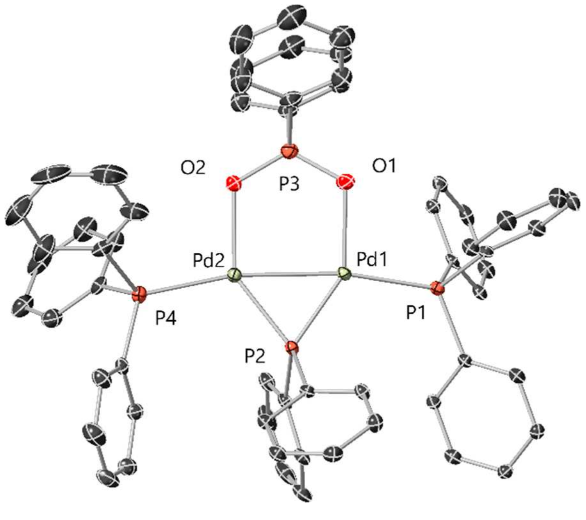

Figure 6. Structure of $[Pd_2(\mu\text{-PPh}_2)\{\kappa_2\text{-O,O-}\mu\text{-P(O)}_2\text{Ph}_2\}(\kappa\text{-PPh}_3)_2]$ (**3**) obtained via a X-ray diffraction of a single crystal grown from THF-d_8 reaction solution of 1 with 2 equiv of PPh_3. Selected interatomic distances /Å Pd1−Pd2 = 2.6140(5) P1−Pd1 = 2.2901(12), Pd2−P4 = 2.3095(12), P2−Pd1 = 2.1810(12), P2−Pd2 = 2.1888(12), Pd1−O1 = 2.162(4), Pd2−O2 = 2.186(4), O1−P3 = 1.507(4), O2−P3 = 1.529(4). Selected interatomic angles /° O1−P3−O2 = 120.7(2), Pd1−P2−Pd2 = 73.48(4). H-atoms not shown.

Analogously to **1** and **2** this complex is bridged by a single μ-diphenylphosphido ligand; however, the secondary bridging ligand is a diphenylphosphinato ligand, which bridges through a κ_2-O_2-μ_2 interaction from the $P(O_2)PPh_2$ moiety. This complex appears to be a rare example, where a phosphinato-type ligand is coordinated to Pd via a bridging interaction through two oxygen atoms. Moissev et al. observed the formation of diphenylphosphinato-bridged Pd^{II} complex, formed from the reaction of $[Pd^{II}(\mu_2\text{-OAc})(\kappa\text{-OAc})(PPh_3)]_2$ with molecular hydrogen in the presence of formic acid.[34] We tentatively propose the presence of **3** as a minor product to be the result of the oxidation of **2** by trace air during the crystallization, a process that is independent of the formation of **2** (Figure 5).

Computational Studies for Complex 2. Computational studies using density functional theory (DFT) calculations for $[Pd^{I}_2(\mu\text{-PPh}_2)\{\kappa_2\text{-P,O-}\mu\text{-P(O)Ph}_2\}(\kappa\text{-PPh}_3)_2]$ **2** were conducted using the B3LYP/DEF2SVP level of theory with an implicit solvent model (SMD, THF implicit solvent) and empirical dispersion corrections (GD3-BJ) (Figure 7). The calculations reveal a short Pd−Pd bond (2.6046 Å), supporting its diamagnetic properties. The HOMO resides on the "Pd−P−O" moiety, whereas the HOMO-1 resides primarily on the

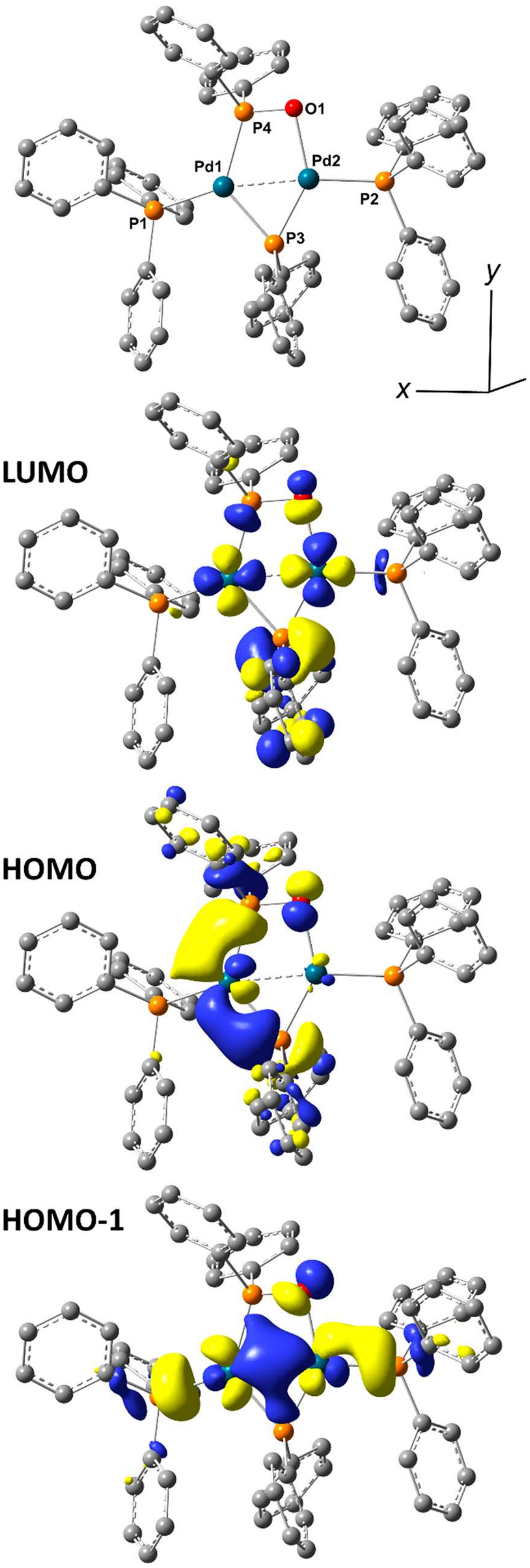

Figure 7. DFT calculated structure of complex **2**, showing the HOMO-1 (P1-Pd1-Pd2-O1-P2 based), HOMO (P3-Pd1-P4-O1 based) and LUMO frontier molecular orbitals.

Pd−Pd centers. The LUMO can be found over the phosphide and Pd−Pd centers. The HOMO and HOMO-1 provide clues about the underlying reactivity of **2** toward other electrophilic species, highlighting that oxidation of the phosphinito to phosphinato being clearly feasible, but also direct reaction of **2** with organohalides (presumably involving HOMO-1), similar to what we revealed for dinuclear Pd complex **1**.[12] Natural bond order (NBO) analysis and calculated Wiberg Indices on complex **2** reveal that there is a reasonable Pd1−Pd2 bonding interaction (see Supporting Information). Wiberg indices for Pd1 and Pd2 were determined to be 0.3167, along with a natural atomic orbital bond order of 0.4737, indicating a partial bond. The Pd2−O1 interaction is relatively weak in comparison to the P4−O1 bond, with Wiberg indices of 0.2697 and 0.9477 respectively. As O1 has a calculated −1 charge, this implies the Pd2−O1 interaction could be more electrostatic than covalent in nature.

Reactivity of the System with 2-Bromopyridine. We next assessed the reactivity and nucleophilicity of both Pd species – $[\mathrm{Pd}^{I}_2(\mu\text{-PPh}_2)\{\kappa_2\text{-P,O-}\mu\text{-P(O)Ph}_2\}(\kappa\text{-PPh}_3)_2]$ **2** and $[\mathrm{Pd}^0(\mathrm{PPh}_3)_3]$ (generated by reaction of two equivalents of PPh_3 with **1**) toward an organohalide, namely 2-bromopyridine. The reason for selecting 2-bromopyridine was that our earlier work[16] had highlighted the challenges associated with characterizing the product(s) of the reaction mixtures of the Pd species between more typical organohalides (e.g., iodobenzene). Furthermore, employing 2-bromopyridine (having a heteroatom) is arguably like substrates that are more typically used by the synthetic chemistry community.

A postreaction mixture of $\mathrm{Pd}^{I}_2(\mu\text{-PPh}_2)\{\kappa_2\text{-P,O-}\mu\text{-P(O)}\text{-Ph}_2\}(\kappa\text{-PPh}_3)_2]$ **2** and $[\mathrm{Pd}^0(\mathrm{PPh}_3)_3]$ was thus treated with an excess of 2-bromopyridine in THF 25 °C. Over a period of 13 h, ^{31}P NMR spectroscopic analysis showed the evolution of several new phosphorus-containing species (Figure 8). Structural assignment was possible for some of the ^{31}P-containing reaction products evolving under the reaction conditions. After 20 min (Figure 8b), the broad signal at δ_P 22.0 ppm, $[\mathrm{Pd}^0(\mathrm{PPh}_3)_3]$, was lost with new resonances forming at δ_P 22.5 and 30.5 ppm and a broad peak at ca. δ_P − 4.4 ppm, which was assigned to liberated PPh_3.

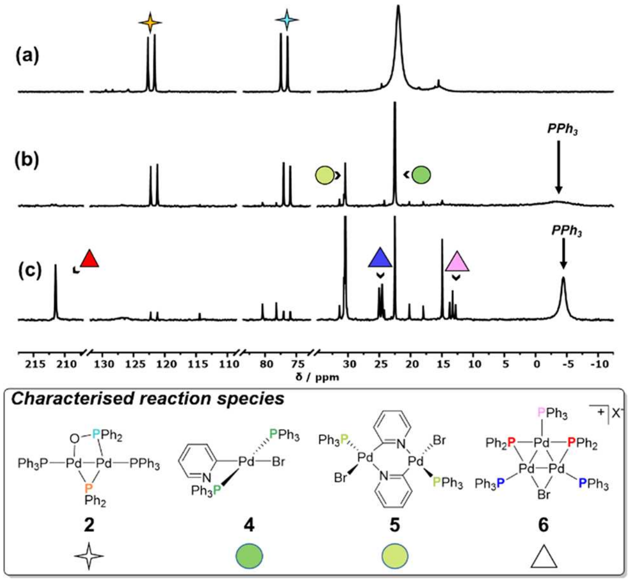

Figure 8. ^{31}P{^{1}H} NMR data (THF-d_8, 25 °C, 203 MHz), recorded as a function of time, for the reaction between the postreaction mixture, generated from **1** and PPh_3, and subsequent reaction with 2-bromopyridine. (a) before, (b) 20 min after, and (c) 13 h after addition of 2-bromopyridine.

The known reaction between $[\mathrm{Pd}^0(\mathrm{PPh}_3)_4]$ and 2-bromopyridine was carried out,[12] which allowed for confirmation of the identity of the resonances at δ 22.5 and 30.5 ppm (see Supporting Information for full details). These resonances are associated with *trans*-$[\mathrm{Pd}^{II}(\mathrm{Br})(\mathrm{N,C}_2\text{-pyridyl})(\mathrm{PPh}_3)_2]$ and *trans*-$[\mathrm{Pd}^{II}(\mathrm{Br})(\mathrm{N,C}_2\text{-pyridyl})(\mathrm{PPh}_3)]_2$, respectively (**4** and **5**); the oxidative addition complexes of 2-bromopyridine to $[\mathrm{Pd}^0(\mathrm{PPh}_3)_2]$, derived from $[\mathrm{Pd}^0(\mathrm{PPh}_3)_3]$,[35] releasing PPh_3 (as observed) in less than 10 min.[36] ESI-MS analysis confirmed the presence of complexes **4** and **5** in the postreaction solution on the basis of observation of the respective *pseudo*-molecular cations $[\mathrm{M}-\mathrm{Br}]^+$.

Unexpectedly, after the addition of 2-bromopyridine, complex **2** was seen to undergo a slower reaction, forming $[\mathrm{Pd}_3(\mu\text{-Br})(\mu\text{-PPh}_2)(\mathrm{PPh}_3)_3]\mathrm{X}$ **6**, with X most likely being diphenylphosphinite $[\mathrm{PPh}_2\mathrm{O}]^-$ or Br^-; the $[\mathrm{Pd}_3(\mu\text{-Br})(\mu\text{-PPh}_2)(\mathrm{PPh}_3)_3]^+$ species was evident by ^{31}P NMR and ESI-MS analysis (Figure 8c). Formation of this particular trinuclear Pd cluster relates to the reactivity of **1** towards 2-bromopyridine, indicating $[\mathrm{Pd}_3(\mu\text{-X})(\mu\text{-PPh}_2)(\mathrm{PPh}_3)_3]\mathrm{X}$ species as a thermodynamic sink promoted by the bromide nucleofuge.[16] We noted that the $\mathrm{Ac}_2\mathrm{O}$ generated in the preceding reaction was left unreacted, while **4**, **5**, and **6** were formed (comparing ^{1}H and ^{31}P NMR analysis).

These findings allow us to fully delineate the reaction pathways for **1**, on reaction with two equivalents of PPh_3, and furthermore 2-bromopyridine, our chosen organohalide to exemplify the link to cross-coupling chemistry (Figure 9).

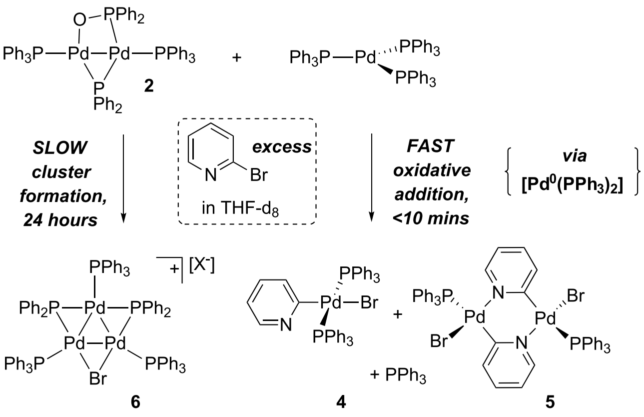

Figure 9. Reactivity of the mixture of Pd^{I} phosphinito complex **2** and $[\mathrm{Pd}^0(\mathrm{PPh}_3)_3]$with 2-bromopyridine.

In conclusion, reaction of $[\mathrm{Pd}^{I}_2(\mu\text{-PPh}_2)(\mu_2\text{-OAc})(\mathrm{PPh}_3)_2]$ **1** with two equivalents of PPh_3 led to disproportionation to $[\mathrm{Pd}^0(\mathrm{PPh}_3)_3]$ and a new complex $[\mathrm{Pd}^{I}_2(\mu\text{-PPh}_2)\{\kappa_2\text{-P,O-}\mu\text{-P(O)Ph}_2\}(\kappa\text{-PPh}_3)_2]$ **2**. The presence of acetic anhydride as a biproduct of the process indicated that the phosphinito ligand had formed by transfer of an oxygen atom via formal acyl transfer to acetate. The crude reaction mixture containing **2** and $[\mathrm{Pd}^0(\mathrm{PPh}_3)_3]$ reacted with 2-bromopyridine at different rates: (1) slowly giving $[\mathrm{Pd}_3(\mu\text{-Br})(\mu\text{-PPh}_2)(\mathrm{PPh}_3)_3]\mathrm{X}$ **6** (formed from **2**); (2) rapidly forming typical oxidative addition products **4** and **5** {formed from $[\mathrm{Pd}^0(\mathrm{PPh}_3)_3]$}. These findings reveal that the unique reactivity of dinuclear Pd^{I} complexes enables access to different Pd speciation, with arguably important implications for cross-coupling catalysis,[37] adding to the complexity of the ubiquitous Pd(OAc)$_2$/nPPh$_3$ precatalyst system.

ASSOCIATED CONTENT

Supporting Information

The Supporting Information is available free of charge at https://pubs.acs.org/doi/10.1021/acs.organomet.1c00347.

Detailed experimental procedures, compound characterization data, and additional supporting data (PDF)

DFT structures (XYZ)

Accession Codes

CCDC 2089316 and 1894929 contains the supplementary crystallographic data for this paper. These data can be obtained free of charge via www.ccdc.cam.ac.uk/data_request/cif, or by emailing data_request@ccdc.cam.ac.uk, or by contacting The Cambridge Crystallographic Data Centre, 12 Union Road, Cambridge CB2 1EZ, UK; fax: +44 1223 336033.

AUTHOR INFORMATION

Corresponding Author

Ian J. S. Fairlamb − *Department of Chemistry, University of York, York, North Yorkshire YO10 5DD, United Kingdom*; Email: ian.fairlamb@york.ac.uk

Authors

Neil W. J. Scott − *Department of Chemistry, University of York, York, North Yorkshire YO10 5DD, United Kingdom*

Mark J. Ford − *Bayer AG, 40789 Monheim, Germany*

David R. Husbands − *Department of Chemistry, University of York, York, North Yorkshire YO10 5DD, United Kingdom*

Adrian C. Whitwood − *Department of Chemistry, University of York, York, North Yorkshire YO10 5DD, United Kingdom*; orcid.org/0000-0002-5132-5468

Complete contact information is available at: https://pubs.acs.org/10.1021/acs.organomet.1c00347

Notes

The authors declare no competing financial interest.

ACKNOWLEDGMENTS

We are grateful to Bayer AG (Ph.D. studentship to N.W.J.S.) for funding this study. D.R.H. is funded by an EPSRC iCASE award (voucher number 19000077) with GlaxoSmithKline. We thank the University of York for supporting NMR spectrometers and X-ray equipment, and EPSRC for NMR upgrades (EP/K039660/1). We thank Karl Heaton (MS), Dr. Alex Heyam and Heather Fish (NMR) for their guidance and support.

REFERENCES

(1) Stambuli, J. P.; Kuwano, R.; Hartwig, J. F. Unparalleled rates for the activation of aryl chlorides and bromides: coupling with amines and boronic acids in minutes at room temperature. *Angew. Chem., Int. Ed.* **2002**, *41*, 4746−4748.

(2) Johansson Seechurn, C. C. C.; Sperger, T.; Scrase, T. G.; Schoenebeck, F.; Colacot, T. J. Understanding the Unusual Reduction Mechanism of Pd(II) to Pd(I): Uncovering Hidden Species and Implications in Catalytic Cross-Coupling Reactions. *J. Am. Chem. Soc.* **2017**, *139*, 5194−5200.

(3) Kalvet, I.; Magnin, G.; Schoenebeck, F. Rapid Room-Temperature, Chemoselective Csp^2−Csp^2 Coupling of Poly(pseudo)-halogenated Arenes Enabled by Palladium(I) Catalysis in Air. *Angew. Chem., Int. Ed.* **2017**, *56*, 1581−1585.

(4) Kalvet, I.; Sperger, T.; Scattolin, T.; Magnin, G.; Schoenebeck, F. Palladium(I) Dimer Enabled Extremely Rapid and Chemoselective Alkylation of Aryl Bromides over Triflates and Chlorides in Air. *Angew. Chem., Int. Ed.* **2017**, *56*, 7078−7082.

(5) Keaveney, S. T.; Kundu, G.; Schoenebeck, F. Modular Functionalization of Arenes in a Triply Selective Sequence: Rapid C(sp^2) and C(sp^3) Coupling of C-Br, C-OTf, and C-Cl Bonds Enabled by a Single Palladium(I) Dimer. *Angew. Chem., Int. Ed.* **2018**, *57*, 12573−12577.

(6) Magnin, G.; Clifton, J.; Schoenebeck, F. A General and Air-tolerant Strategy to Conjugated Polymers within Seconds under Palladium(I) Dimer Catalysis. *Angew. Chem., Int. Ed.* **2019**, *58*, 10179−10183.

(7) Murahashi, T.; Nagai, T.; Okuno, T.; Matsutani, T.; Kurosawa, H. Synthesis and ligand substitution reactions of a homoleptic acetonitrile dipalladium(I) complex. *Chem. Commun.* **2000**, 1689−1690.

(8) Han, X.; Weng, Z.; Hor, T. S. A. Suzuki coupling catalyzed by a homoleptic Pd(I)−Pd(I) solvento complex. *J. Organomet. Chem.* **2007**, *692*, 5690−5696.

(9) Fricke, C.; Sperger, T.; Mendel, M.; Schoenebeck, F. Catalysis with Palladium(I) Dimers. *Angew. Chem., Int. Ed.* **2021**, *60*, 3355.

(10) Amatore, C.; Jutand, A.; M'Barki, M. A. Evidence of the Formation of Zerovalent Palladium from Pd(OAc)$_2$, and Triphenylphosphine. *Organometallics* **1992**, *11*, 3009−3013.

(11) Amatore, C.; Carre, E.; Jutand, A.; M'Barki, M. A. Rates and Mechanism of the Formation of Zerovalent Palladium Complexes from Mixtures of Pd(OAc)$_2$ and Tertiary Phosphines and Their Reactivity in Oxidative Additions. *Organometallics* **1995**, *14*, 1818−1826.

(12) Amatore, C.; Jutand, A. Anionic Pd(0) and Pd(II) intermediates in palladium-catalyzed Heck and cross-coupling reactions. *Acc. Chem. Res.* **2000**, *33*, 314−321.

(13) Kirlikovali, K. O.; Cho, E.; Downard, T. J.; Grigoryan, L.; Han, Z.; Hong, S.; Jung, D.; Quintana, J. C.; Reynoso, V.; Ro, S.; Shen, Y.; Swartz, K.; Ter Sahakyan, E.; Wixtrom, A. I.; Yoshida, B.; Rheingold, A. L.; Spokoyny, A. M. Buchwald−Hartwig amination using Pd(I) dimer precatalysts supported by biaryl phosphine ligands. *Dalton Trans.* **2018**, *47*, 3684−3688.

(14) Wagschal, S.; Perego, L. A.; Simon, A.; Franco-Espejo, A.; Tocqueville, C.; Albaneze-Walker, J.; Jutand, A.; Grimaud, L. Formation of XPhos□Ligated Palladium(0) Complexes and Reactivity in Oxidative Additions. *Chem. - Eur. J.* **2019**, *25*, 6980−6987.

(15) Montgomery, M.; O'Brien, H. M.; Méndez-Gálvez, C.; Bromfield, C. R.; Roberts, J. P. M.; Winnicka, A. M.; Horner, A.; Elorriaga, D.; Sparkes, H. A.; Bedford, R. B. The surprisingly facile formation of Pd(I)−phosphido complexes from ortho-biphenylphosphines and palladium acetate. *Dalton Trans.* **2019**, *48*, 3539−3542.

(16) Scott, N. W.; Ford, M. J.; Schotes, C.; Parker, R. R.; Whitwood, A. C.; Fairlamb, I. J. The ubiquitous cross-coupling catalyst system 'Pd(OAc)$_2$'/2PPh$_3$ forms a unique dinuclear Pd I complex: an important entry point into catalytically competent cyclic Pd$_3$ clusters. *Chem. Sci.* **2019**, *10*, 7898−7906.

(17) Coulson, D. R. Ready cleavage of triphenylphosphine. *Chem. Commun. (London)* **1968**, 1530−1531.

(18) Berenblyum, A. S.; Aeeva, A. P.; Lakhman, L. I.; Moiseev, I. I. Mechanism of the formation of palladium complexes serving as catalysts in hydrogenation reactions. *J. Organomet. Chem.* **1982**, *234*, 237−248.

(19) Fu, F.; Xiang, J.; Cheng, H.; Cheng, L.; Chong, H.; Wang, S.; Li, P.; Wei, S.; Zhu, M.; Li, Y. A Robust and Efficient Pd3 Cluster Catalyst for the Suzuki Reaction and Its Odd Mechanism. *ACS Catal.* **2017**, *7*, 1860−1867.

(20) Diehl, C. J.; Scattolin, T.; Englert, U.; Schoenebeck, F. C-I Selective Cross-Coupling Enabled by a Cationic Pd Trimer. *Angew. Chem., Int. Ed.* **2019**, *58*, 211−215.

(21) Proutiere, F.; Schoenebeck, F. Solvent Effect on Palladium-Catalyzed Cross-Coupling Reactions and Implications on the Active Catalytic Species. *Angew. Chem., Int. Ed.* **2011**, *50*, 8192−8195.

(22) Proutiere, F.; Aufiero, M.; Schoenebeck, F. Reactivity and stability of dinuclear Pd(I) complexes: studies on the active catalytic species, insights into precatalyst activation and deactivation, and application in highly selective cross-coupling reactions. *J. Am. Chem. Soc.* **2012**, *134*, 606−612.

(23) Aufiero, M.; Scattolin, T.; Proutière, F.; Schoenebeck, F. Air-Stable Dinuclear Iodine-Bridged Pd(I) Complex - Catalyst, Precursor, or Parasite? The Additive Decides. Systematic Nucleophile-Activity Study and Application as Precatalyst in Cross-Coupling. *Organometallics* **2015**, *34*, 5191−5195.

(24) Hruszkewycz, D. P.; Balcells, D.; Guard, L. M.; Hazari, N.; Tilset, M. Insight into the efficiency of cinnamyl-supported precatalysts for the Suzuki-Miyaura reaction: observation of Pd(I) dimers with bridging allyl ligands during catalysis. *J. Am. Chem. Soc.* **2014**, *136*, 7300−7316.

(25) Vilar, R.; Mingos, D. M. P.; Cardin, C. J. Synthesis and structural characterisation of $[Pd_2(\mu\text{-}Br)_2(PBut_3)_2]$, an example of a palladium(I)−palladium(I) dimer. *J. Chem. Soc., Dalton Trans.* **1996**, 4313−4314.

(26) Dura-Vila, V.; P. Mingos, D.M.; Vilar, R.; White, A. J.P.; Williams, D. J. Reactivity studies of $[Pd_2(\mu\text{-}X)_2(PBut_3)2]$ (X = Br, I) with CNR (R = 2,6-dimethylphenyl), H2 and alkynes. *J. Organomet. Chem.* **2000**, *600*, 198−205.

(27) Arif, A. M.; Heaton, D. E.; Jones, R. A.; Nunn, C. M. Di- and trinuclear di-tert-butylphosphido-bridged complexes of palladium. Synthesis and x-ray structures of $[Pd(\mu\text{-tert-}Bu_2P)(PMe_3)]_2$(Pd-Pd) and mixed-valence $Pd_3(\mu\text{-tert-}Bu_2P)(CO)_2Cl$. *Inorg. Chem.* **1987**, *26*, 4228−4231.

(28) Al-Farhan, K. A. Crystal structure of triphenylphosphine oxide. *J. Crystallogr. Spectrosc. Res.* **1992**, *22*, 687−689.

(29) Matt, D.; Ingold, F.; Balegroune, F.; Grandjean, D. Reactivity of phosphine-phosphinite complexes. synthesis and crystal structure of $[\{Ph_2PCHC(O)Ph\}Pd(\mu\text{-}Ph_2PO)]_2$. *J. Organomet. Chem.* **1990**, *399*, 349−360.

(30) (a) Gallo, V.; Latronico, M.; Mastrorilli, P.; Nobile, C. F.; Suranna, G. P.; Ciccarella, G.; Englert, U. Synthesis of Phosphido-Bridged Phosphinito Platinum(I) Complexes by Reaction of cis-$PtCl_2(PHCy_2)_2$ with Oxygenated Bases − Crystal Structure of $[(PCy_2OMe)Pt(\mu\text{-}PCy_2)]_2$(Pt−Pt). *Eur. J. Inorg. Chem.* **2005**, *2005*, 4607−4616. (b) Arias, A.; Fornies, J.; Fortuno, C.; Ibanez, S.; Martin, A.; Mastrorilli, P.; Gallo, V.; Todisco, S. Addition of Nucleophiles to Phosphanido Derivatives of Pt(III): Formation of P-C, P-N, and P-O Bonds. *Inorg. Chem.* **2013**, *52*, 11398−11408.

(31) Edwards, D. A.; Hayward, R. N. Transition metal acetates. *Can. J. Chem.* **1968**, *46*, 3443−3446.

(32) Rosenberg, L. Metal complexes of planar PR_2 ligands: Examining the carbene analogy. *Coord. Chem. Rev.* **2012**, *256*, 606−626.

(33) Barnett, B. R.; Labios, L. A.; Stauber, J. M.; Moore, C. E.; Rheingold, A. L.; Figueroa, J. S. Synthetic and Mechanistic Interrogation of Pd/Isocyanide-Catalyzed Cross-Coupling: π-Acidic Ligands Enable Self-Aggregating Monoligated Pd(0) Intermediates. *Organometallics* **2017**, *36*, 944−954.

(34) Moiseev, I. I.; Stromnova, T. A.; Busygina, I. N.; Tihonova, N. Y.; Kozitsyna, N. Y.; Ellern, A. M.; Antipin, M. Y.; Struchkov, Y. T. Oxidation of bridging groups by carboxylate coordinated ligands in palladium clusters. *J. Cluster Sci.* **1992**, *3*, 411−421.

(35) Fauvarque, J.-F.; Pflüger, F.; Troupel, M. Kinetics of oxidative addition of zerovalent palladium to aromatic iodides. *J. Organomet. Chem.* **1981**, *208*, 419−427.

(36) Maes, B. U. W.; Verbeeck, S.; Verhelst, T.; Ekomié, A.; von Wolff, N.; Lefèvre, G.; Mitchell, E. A.; Jutand, A. Oxidative Addition of Haloheteroarenes to Palladium(0): Concerted versus SNAr-Type Mechanism. *Chem. - Eur. J.* **2015**, *21*, 7858−7865.

(37) Scott, N. J. W.; Ford, M. J.; Jeddi, N.; Eyles, A.; Simon, L.; Whitwood, A. C.; Tanner, T.; Willans, C. E.; Fairlamb, I. J. S. A Dichotomy in Cross-Coupling Site Selectivity in a Dihalogenated Heteroarene: Influence of Mononuclear Pd, Pd Clusters, and Pd Nanoparticles—the Case for Exploiting Pd Catalyst Speciation. *J. Am. Chem. Soc.* **2021**, *143*, 9682−9693.